Experimental results from the Cadarache 1 MV test bed with SINGAP accelerators

L Svensson, D Boilson*, H P L de Esch, R S Hemsworth, and A Krylov,
Association EURATOM-CEA, CEA/DSM/DRFC, CEA-Cadarache,
13108 ST PAUL-LEZ-DURANCE (France)
Association EURATOM-DCU , PRL/NCPST, Glasnevin, Dublin 13, Ireland

Abstract

A prototype accelerator based on a pre-accelerator normally used for positive ion acceleration was used on the Cadarache MV negative ion beam facility up to 2004. Even though this accelerator demonstrated the feasibility of SINGAP (SINgle GAP, SINGle APerture) accelerators it was not possible to produce beams with the optical quality required for ITER. A new “ITER-like” accelerator, which is a scaled down version of the ITER SINGAP accelerator, has been built and installed on the Cadarache 1 MV test bed. The objective with the “ITER-like” is to demonstrate reliable D^- beam acceleration as close as possible to 1 MeV with a current density $\bar{j} \approx 200$ A/m^2 with the beam optics required for ITER, i.e. a beamlet divergence of ≤ 7 mrad and beamlet steering within ± 2 mrad of that specified. High voltage hold-off tests have been performed and 940 kV has been held without breakdowns. Beams up to 850 keV (D^-, 15 A/m^2) were obtained after 4 weeks of experiments and the highest current density that has been obtained so far is 150 A/m^2 (D^-, 580 keV). The required beam optics for ITER has been obtained but a larger than expected halo has been measured.

Introduction

The European concept for a 1 MeV, 40 A negative ion based accelerator for the neutral beam system on ITER, the SINgle GAP, SINGle Aperture (SINGAP), is an attractive alternative to the ITER reference design, the so-called MAMuG (Multi-Aperture, Multi-Grid) accelerator. A prototype SINGAP accelerator has been used for several years and produced D^- beams of 910 keV, 30 A/m^2 [1]. The measured beam profiles on the target agreed well with those predicted by calculations. However with the prototype accelerator it was not possible to produce beams with the optical quality required for ITER [2], [3], i.e. a beamlet divergence of ≤ 7 mrad and beamlet aiming within ± 2 mrad of that specified. Therefore a new accelerator has been designed and built in order to demonstrate that the beam optics required for ITER can be achieved with a SINGAP accelerator.

The SINGAP testbed

The Cadarache 1 MV negative ion beam facility is capable of accelerating 100 mA of H^- or D^- up to 1 MeV. The negative ions are first accelerated in the pre-accelerator to energies of 10-50 keV and thereafter up to 1 MeV in the post-accelerator. The ion source is at ground potential and the negative ion beam is extracted and accelerated up to high positive potential and stopped on the calorimeter, which is at the same high potential. The calorimeter is made of 19 mm thick Mitsubishi MFC1-A graphite, which has a much higher thermal conductivity in the beam direction than in the orthogonal directions. The beam footprint is measured at the rear of the target with an IR camera. A detailed description of the test bed can be found in [1].

The accelerator

The first type of pre-accelerator that was used on the Cadarache MV test bed featured a very long “kerb” formed by its deep pre-acceleration grid support system and its cylindrical extension piece. That structure created (1) an electrostatic equipotential drift space before the post acceleration took place and (2) a strong electrostatic lens, which caused all the beamlets to cross over. The required beam optics necessary for ITER, could not be met with this arrangement.

The “ITER-like” pre-accelerator consists of a plasma grid, an extraction grid and a pre-acceleration grid. The pre-acceleration gap is 20 mm. The standard extraction gap is 3 mm, but we also performed experiments with a 6 mm extraction gap. Each grid and its associated water tubes are embedded in a circular stainless steel (SS) grid support plate. These plates are mounted on alumina post insulators from a common SS base plate. This arrangement makes it easy to modify the spacing between the grids by simply inserting shims between the post insulators and the SS base plate. The extraction grid and the pre-acceleration grid have aperture patterns of 5 x 5 with a horizontal and vertical pitch of 20 mm. Each aperture is 14 mm in diameter and its surface area is 1.54 cm^2. A 20 mm high “kerb” made of stainless steel is fitted at the exit of the pre-accelerator. The kerb modifies the electrostatic potential such that the outer beamlets are deflected towards the beam centre whilst traversing the post-acceleration gap. A cross section of the “ITER-like” accelerator with the ion source can be seen in figure 1.

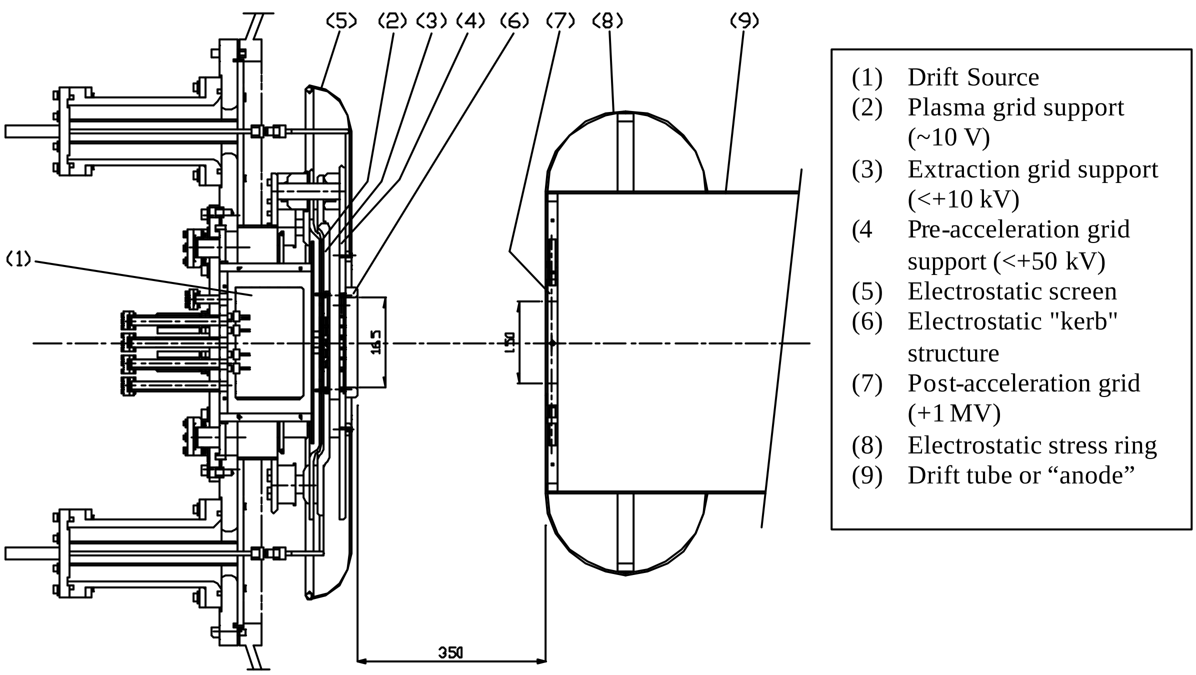

Figure 1. Vertical section of the “ITER-like” SINGAP beam source.

The Cadarache 1 MV power supply has a current limit of 100 mA, which limits the numbers of apertures on the plasma grid to 3 when 200 A/m^2 beams are to be produced. The plasma grid has two thermocoax heater elements embedded in the source side of the grid. This enables heating of the plasma grid to ≈300 °C for efficient negative ion production with Cs seeding of the source [4]. The extraction grid and the pre-acceleration grid are both water cooled through horizontal channels between the aperture rows and incorporate CoSm magnets for electron suppression and/or ion trajectory correction. A schematic of the grids with their water channels and the magnets is shown in figure 2. The beamlets formed in the pre-accelerator are accelerated to ≤1 MeV in one step across the main acceleration gap of 350 mm. The post-acceleration grid has only one large square opening, 150 x 150 mm^2, and is made of OFHC copper. It can be displaced vertically and horizontally, thus providing aperture offset beam steering to simulate the vertical steering (±0.55°) required on ITER or just for correction of misalignment.

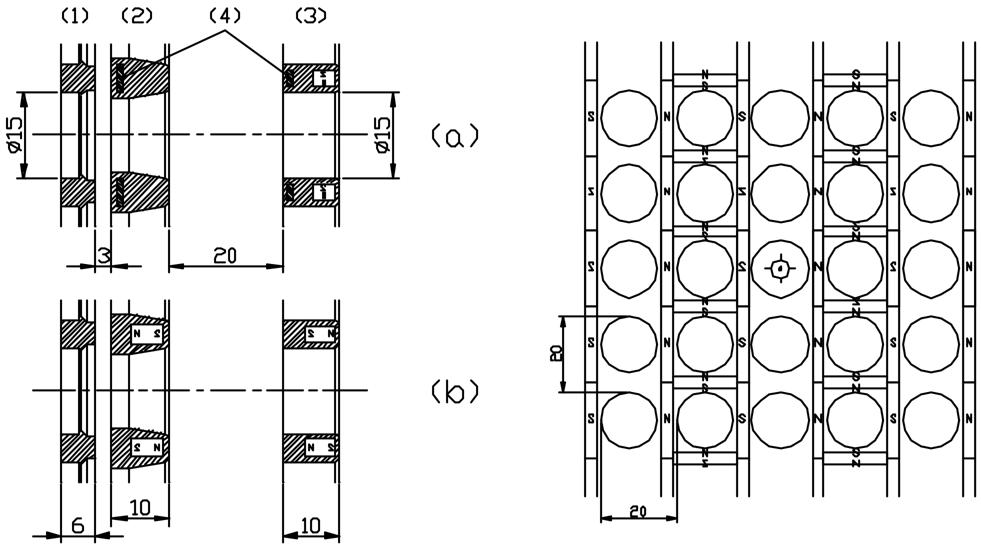

Figure 2. The pre-accelerator aperture geometry is shown on the left: (a) vertical (b) horizontal cut. (1) plasma grid, (2) extraction grid, (3) pre-acceleration grid, (4) water channels. On the right one can see the magnet configuration in the pre-acceleration grid.

Experimental results and comparison with simulations

1. Voltage holding

A resistor is installed in series with the MV power supply in order to limit the current in case of a break down in the accelerator. The original value of this resistor was 1 Mohm and it had an energy limit of 20 kJ per shot, which limited the pulse length to 2 seconds at 100 mA of current. It was replaced by a 110 kOhm high power resistor at the same time as the new "ITER-like" accelerator was installed on the MV test bed. The new resistor is not any longer imposing a pulse length restriction at 100 mA but in practice the pulse length is restricted by the existing timing system, to 40 s. It is found that with the extended pulse length the operating time required to condition the accelerator is drastically reduced.

On application of high voltage to the system with no gas flowing and no discharge in the ion source the so-called "dark current" appears, the cause of which is not known [5]. This dark current flows from the ground potential structure (mainly the vacuum vessel walls) to the structure at high voltage. The long pulse lengths, that are now available with the high power series resistor, result in substantial heating of the drift tube and its support structure by the dark current and some hot spots have been observed. The dark current is reduced by increased background pressure in the vacuum vessel. The pressure that is needed to suppress the dark current for the different configurations so far used is shown in table 1. In principle any gas can be used but helium is favoured, since the cryo-sorption pump installed on the vacuum vessel does not pump it. The pressure needed to suppress the dark current with the ITER-like accelerator is higher than the predicted pressure around the accelerator of the ITER injector (0.03 Pa) [6]. The reason for this high pressure with the "ITER-like" accelerator compared with the prototype accelerator with 350 mm gap is not known.

Type of accelerator configuration	Type of gas	Pressure	Achieved breakdown free HV pulses
Prototype accelerator with 625 mm acceleration gap	Helium	0.017 Pa	1000kV
Prototype accelerator with 350 mm acceleration gap	Helium	0.03 Pa	940 kV
	Deuterium	0.034 Pa	
ITER-like accelerator with 350 mm acceleration gap	Helium	0.07 Pa	940 kV
	Deuterium	0.07 Pa	

Table 1. The pressures needed to suppress the dark current and the achieved breakdown free high voltage for the different types of accelerators tested at the MV testbed.

Breakdown free HV pulses up to 940 kV were achieved for all three accelerators after only 160 minutes of accumulated voltage on time. Higher voltages for the configurations with 350 mm gap have not been attempted in order to minimise the risk of breakdowns at higher voltages damaging the 1 MV power supply.

2. Introduction to beam optics experiments

Originally the prototype accelerator had 11 apertures in the pre-accelerator and a main acceleration gap of 625 mm. This was later reduced to 350 mm since calculations showed that 350 mm was required to obtain good beam optics for ITER. The 350 mm main acceleration gap led, as expected, to a stronger electrostatic lens at the exit of the pre-accelerator. The resulting increase in the electric field increased the strength of the lens at the exit of the pre-accelerator and as a consequence the beamlets crossed closer to the accelerator than had been the case with the longer (625 mm) gap. Since the lens strength increases with the acceleration field, the cross over moved towards the accelerator as the beam energy was increased. An upper limit was reached when the outer beamlets fell outside the carbon target. To avoid this the aperture array was masked so that only the central 4 apertures were open. With this arrangement beams with energy of 916 keV were produced with a current density measured at the target of 50 A/m^2. The dark current was suppressed almost completely by raising the pressure in the vacuum tank to ≈ 0.03 Pa. In general a good agreement was found between the measured and predicted footprints on the target.

With the new “ITER-like” accelerator, initially three apertures were used for beam acceleration as then with the 100 mA available from the MV power supply we should have been able to accelerate a current density of 200 A/m^2. This proved not to be the case as it was found that a substantial fraction (≈40 %) of the current taken from the MV power supply was not reaching the beam target. As it could not be established where the power was being lost, a second phase of the operation was therefore devoted to single beamlet operation in order to allow the beamlet optics to be investigated in more detail over a larger range of current densities.

One reason for the poor transmission could be back streaming positive ions that had been created downstream of the pre-accelerator. The positive ions that are created are either D^+, D_2^+ or He^+ in the cases helium has been used as gas to suppress the dark current. In an attempt to suppress the extraction of positive ions from the drift tube, (see figure 1) a positive ion suppression filter made of permanent magnets has been installed 150 mm downstream of the post acceleration grid. The filter strength is 430 gauss×cm perpendicular to the beam direction.

Using this accelerator an "ITER-relevant" shot is defined as a shot that is run at:
(1) the same perveance as required for ITER (1MeV, 200 A/m^2 D$^-$ on the target).
(2) using a pre-acceleration scheme that produces beam divergence acceptable to ITER [8].
It is expected that the pre-acceleration scheme that produces large diameter converging beamlets [2] will be ITER-relevant. The optics of ITER-relevant shots was evaluated at lower energy and current, but at the correct perveance.

3. Optics calculations and measurements of the beam footprints

The beam optics calculation and simulation of the measured beam profiles has been described in detail in [2] and [7]. An addition to the previously described procedure is that the calculated temperature profiles now include the time and temperature dependent 3D heat diffusion occurring during the transit from the exposed front towards the rear face of the carbon target where the temperature distribution is measured experimentally with an infrared camera.

The calorimetric measurements of the beam footprints are measured with an infrared camera system. Previously these measurements were made with an AGEMA thermovision 782 system but this has been replaced with a more modern camera type, a FLIR 550. The better temperature and spatial resolution of the new camera has made it possible to more accurately measure the power of the beam hitting the calorimeter and to reveal the presence of beam halos.

4. Operation with 3 apertures

The first comparisons between simulations and experiments were done for shot 7545. This shot had 1.8 s of 28 A/m^2 D$^-$ beams, 13 mA in total, as determined from the energy deposited onto the target. Taking stripping losses into account, the extracted current density from the source was 36 A/m^2. The extraction voltage was 2.5 kV, the pre-acceleration voltage 18 kV and the post-acceleration voltage 625 kV. The source pressure was 0.4 Pa, the plasma grid was at 225 °C and the source was caesiated. The result of the simulation can be seen on the right in figure 3 and the measured infrared data is shown on the left. This shot was chosen for the simulation because the three beamlets are well resolved, which facilitates the detailed comparison with the simulations which include the magnetic fields present in the system.

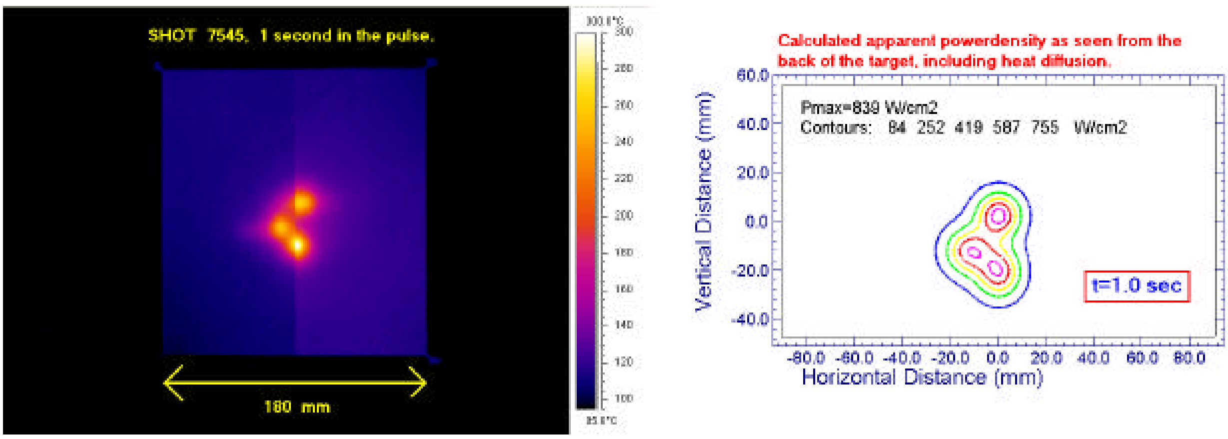

Figure 3. Infra red data taken from the back of the carbon target for shot 7545 (28 A/m^2 D$^-$) is shown on the left. The calculated power density is shown on the right.

We see from the data in figure 3:

- The two beamlets on the right are vertically 30 mm apart (the calculation gives 23 mm).
- The lower two beamlets are horizontally 11 mm apart (the calculation gives 12 mm).
- The power density profile is wider than calculated, but the central part not by very much.

The reason why the beamlets are vertically further apart than calculated is not yet clear.

With the experimental profile information available, we have tried to determine the actual beam optics. If we assume that the starting positions of the beamlets are correct and adjust the steering angles to match the measured positions on the target, the beamlet positions at the target will be correct, but the current density will still be too high. The measured power density indicates that the beamlet optics are worse than those calculated; either the beamlet divergence is higher than calculated, or the beamlet profile is not the assumed simple Gaussian. Simply degrading the beamlet divergence to match the peak power density results in calculated profiles that are too narrow at the edge and too wide in the centre (smearing out the individual beamlets). A reasonable match can be found if it is assumed that the beamlet profile is bi-Gaussian with 60% with a divergence of $\approx$3 mrad and 40% with a 7 mrad divergence.

5. Single aperture beam halo studies

The possibility was considered that operating in Cs could cause a much larger halo than operating in "volume". There are two possible reasons for this:
(1) Non-uniform D^- flux over the 14 mm diameter aperture.
(2) It is likely that surfaces on the extraction and pre-acceleration grids become covered with caesium. Escaping D^0 from the source could be converted to D^- on these surfaces. Simulations indicate that $\approx$40 % of these D^- ions would escape from the surface and be accelerated, but with very bad beam optics.

If either of these processes plays a significant role, then operation of the ion source in "volume" should show a much smaller halo than with caesium operation. Therefore dedicated experiments have therefore been carried out to assess if this is the case.

To quantify the stripping losses in the SINGAP accelerator and to measure the halo's in "volume", two experiments were done with a different amount of deuterium background gas in the tank. The average of ten identical shots was taken and the vertical Gaussian fit of the beam profile was analyzed. In the case of low pressure in the tank (P=0.01Pa, shots 8918 – 8927), the main beam has a divergence that is better than 7 mrad and the (rather poorly determined) width of the halo is 80 mm, which corresponds to a divergence of $\approx$ 30 mrad. The fraction of power in the halo is 14% and 4.8 % of the beam current is calculated to be lost as stripping losses. These shots were performed at 226 kV at which voltage the dark current is zero and it is unnecessary to add gas to suppress the dark current. The thermal current on target was 1.6 mA. The transmission, defined as thermal current / electrical drain current from the MV power supply is calculated to be 80%.

The results from operation with high pressure (P=0.09 Pa, shots 8932 - 8941) in the tank are shown in table 2. Apart from the high tank pressure, these shots are identical to the low-pressure shots described above. The stripping losses are calculated to be 38 %. The transmission (Ithermal / Idrain), is only 30 % compared with 80 % when we had low pressure in the tank. When comparing the two pressures scans we can see that there is no significant effect from stripping losses on the beam halo. This feature can be explained from the simulation that shows that an individual beamlet has a small divergence / convergence over most of its trajectory inside the post-accelerator and its loss by stripping leaves the newborn neutral part of the main beam.

Table 2 also shows the results from various shots that have been analyzed in detail. The “volume” shots were done with a perveance slightly higher than an “ITER-relevant” shot, whereas the Cs shots were all “ITER-relevant”. (See definition of “ITER-relevant” in section 2). All these shots were done with the positive ion suppression filter 150 mm down stream of the post acceleration grid installed. A part of the beam footprint falls off the target as a reduced size target was used in this campaign (95 x 190 mm). The fraction that is missing the target is calculated and included in table 2.

Shot	J thermal A/m^2	Time (s)	Ptank (Pa)	HALO	Stripp-ing loss	Fraction missing the target	Trans-miss-ion	Power account-ability
Volume 8918-8927	10.5	3.0	0.01 D_2	14%	4.8%	7.5%	80%	91%
Volume 8932-8941	7.5	3.0	0.09 D_2	14%	38%	7.5%	30%	53%
Cs 9023	25	3.0	0.002 D_2	27%	1%	14%	76%	89%
Cs 9081	66	1.5	0.07 He	29%	14%	14%	65%	88%
Cs 9091	71	1.5	0.075 He	29%	14%	14%	60%	81%
Cs 9310	67	1.0	0.085 He	30%	15%	8%	~54%	~70%
Cs 9319	63	0.9	0.095 He	28%	17%	8%	~50%	~65%
Volume 9542-9554	6.0	3.2	0.005 D_2	13%	2%	8.4%	69%	76%
Volume 9625-9640	7.2	3.1	0.003 D_2	15%	1%	6.5%	72%	78%
Cs 9712	64	1.1	0.05 He	31%	11%	9%	~60%	~74%
Cs 9752	63	1.1	0.04 He	28%	8%	6%	~63%	~73%

Table 2. “ITER-relevant” shots performed with the positive ion suppression filter 150 mm down stream of the post acceleration grid. The "power accountability" is the transmission corrected for the power missing the target and the stripping losses in the main acceleration gap relative to grid-3. All stripping losses quoted in the table are the losses in the main acceleration gap only.

We can conclude from the data presented in table 2 that:

(1) The halo in the volume shots is around 15 %. The halo for the caesiated shots, which are all “ITER-relevant”, is around 30 % of the total beam power.

(2) Beam transmission and power accountability (defined as the power transmitted to the target + power missing the target + stripping losses in main acceleration gap) decrease strongly with increasing tank pressure.

Dedicated experiments to measure the transmission as a function of pressure are described in the next section. Here we conclude that the premise that caesium causes an increased halo cannot be discarded.

The halo in a short pulse appears to be larger than in long pulses. This could be due to the long ramp-up time (approx. 100 ms) of the MV power supply. During that period the beam is not in perveance match.

Operation without the positive ion suppression filter downstream of the post acceleration grid was done before the shots presented above. Unfortunately during that campaign we did not run at optimum perveance and it makes it difficult to do a direct comparison between shots done with or without the positive ion suppression filter. Some indications show however that the halo without the filter could be up to 40 % of the power intercepted on the target.

6. Beam transmission and pressure scans

Several pressure scans, one of which is shown in figure 4, all show that the electrical drain current increases with pressure and the thermal current decreases with pressure. Our preliminary conclusion is that the reduction in thermal current on the target with increasing pressure in the vacuum vessel is due to the stripping losses. See figure 4. The increase in Idrain might be explained by back streaming positive ions created by ionisation of the background gas. Some ionisation will always occur and it should be kept in mind that whereas stripping is relevant over 350 mm, ionisation of background gas is relevant over at least 500 mm due to field penetration inside the anode. The effect could be amplified by back streaming positive ions ionising the background gas and to emission of secondary electrons when they hit the pre-accelerator. As not all the cross-sections involved are known, this cannot be quantified.

Several pressure-variation experiments have been conducted and they all show a reduction in thermal current and an increase in drain current at higher pressure. The effect is twice as strong in deuterium compared with helium. D_2 has two atoms per molecule and cross-sections that are a factor of two higher than for helium. Two of these experiments are shown in figure 5.

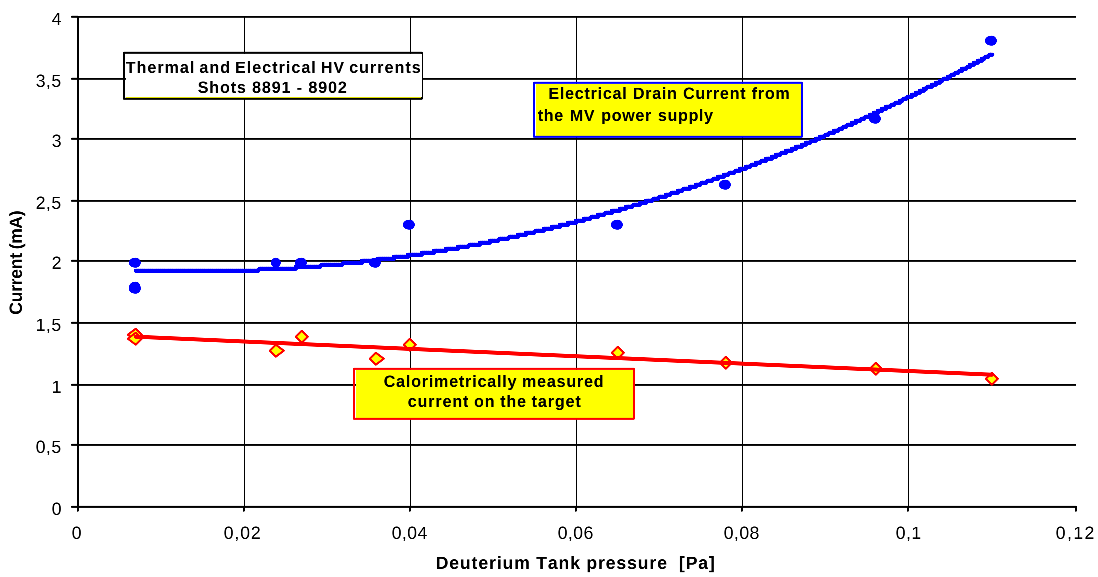

Figure 4. The thermal and electrical drain current from the MV power supply for different tank pressures. Deuterium was used in these shots.

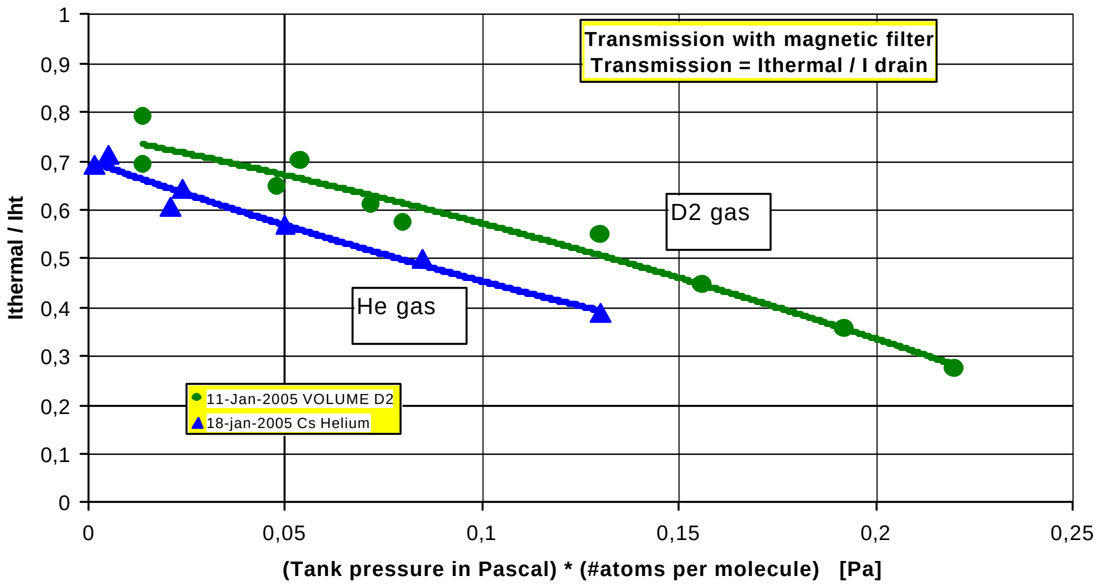

Figure 5. The transmission measured for two different series of pressure scans.

7. Beam optics scan

In section 5 we established from the thermographic measurements on the graphite target that in caesium operation ~70% beam power is contained in a narrow beam and ~30% of the beam power is in a halo. An experiment was conducted to find the best beam-optics under ITER-relevant conditions. At three different values of the extraction voltage, the pre-acceleration voltage V_{pre} was varied and single-Gaussian fits to the experimental data were made. The experiments at the extraction voltage V_{ext}=3.0 kV were done with a deuterium current density j_D^- = 65 A/m^2 measured on the target and a post-acceleration voltage V_{post}=495 kV. The experiments at j_{ext}=2.7 and 3.3 kV were done at the slightly lower current density of j_D^- = 60 A/m^2 and the same V_{post}. The source pressure was 0.4 Pa and 0.09 Pa of helium was added to suppress dark currents. Figure 6 gives the horizontal 1/e half width of the scans, obtained by fitting a single Gaussian to the measured power-density profile.

A clear minimum width is present for V_{ext}=3.0 kV and V_{pre}=20 kV. These are exactly the expected operating voltages for the ITER accelerator at V_{post}=500 kV [2] and [3]. The corresponding current density, however, is 70 A/m^2 D$^-$. Because the pressure was high, the current density in the pre-accelerator certainly had the correct value.

The measured 1/e half width of the beam at optimum perveance was 17 mm horizontally and 20 mm vertically. This is a profile measured 1 second after the end of the beam pulse. Simulations with a heat diffusion code show that the input power density would have had a horizontal half width of 14.5 mm and a vertical half width of 18.5 mm.

The distance between the post-acceleration grid and the target is 2.73 metres. It is assumed that space charge compensation starts 0.11 m downstream of this grid. From that point on, the beamlet is assumed to (1) have a radius no smaller than 5 mm, (2) expand linearly towards the target that is 2.62 metres downstream. Simulations have shown that under a very wide range of conditions, the beamlet cannot be narrower than 5 mm in radius at the SINGAP post-acceleration grid.

Therefore, the best horizontal ITER-relevant divergence is (14.5-5.0)/2.62 = 3.6 mrad. Similarly, the best vertical ITER-relevant divergence is (18.5-5.0)/2.62 = 5.2 mrad. These values are acceptable to ITER with margin. Quite often the beam profiles are elliptical, as is indeed the case here. The most likely reason for this are the magnetic fields in the system, which all act in the vertical direction.

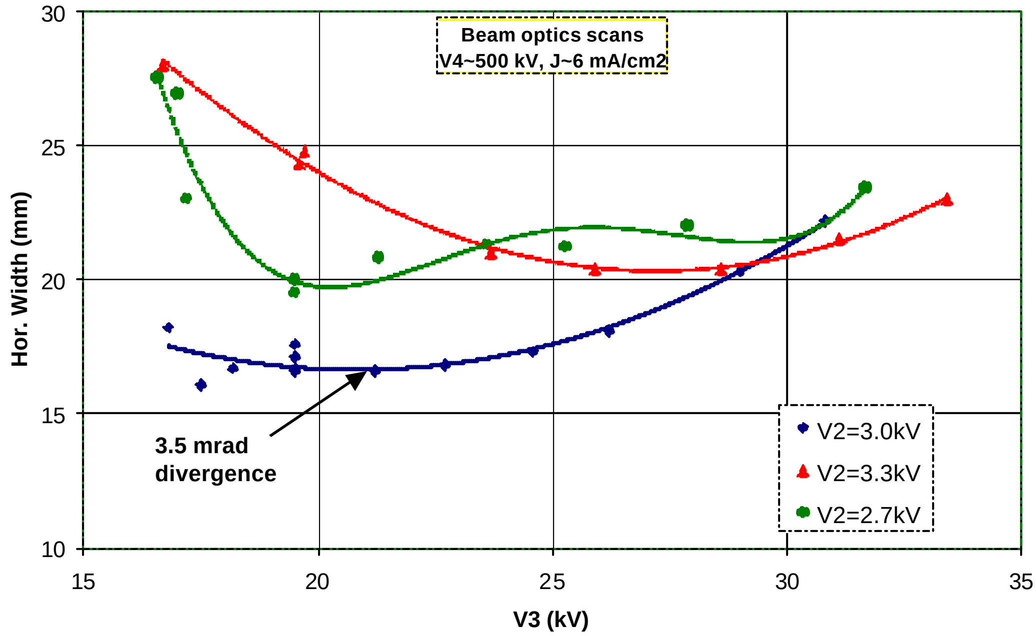

Figure 6. Measurements of the horizontal beam width are plotted for different pre-accelerator voltages.

8. Aperture offset steering

ITER requires the possibility to move the beam between on-axis and off-axis plasma heating. The required steering angle is ±10 mrad. With the SINGAP accelerator this beam steering can be achieved by simply displacing the post acceleration grid vertically without moving the pre-accelerator. A dedicated experiment was set up and the footprint measured on the target can be seen in figure 7. The footprint on the left shows the three beamlets well aligned. The post acceleration grid was thereafter displaced 16 mm to the left (viewed along the beam direction from the ion source). The calculated shift on the target should be 32 mm which corresponds to a steering of 12 mrad. The measurement of the shift of the footprint gave 32 mm as calculated. The wider profile on the right in figure 7 is related to the beam optics, not to the anode displacement.

9. Study of sensitive beam optics

During operation of the ITER-like accelerator a remarkable feature is observed. The beamlet can flip between a peaked power density profile and a hollow density profile. This can happen due to a very modest change (10 %) of extraction voltage, arc current / voltage or bias. The reason for this is not fully understood and is still under investigation. One explanation could be that the plasma is falling off the knife-edge on the plasma grid. Figure 8 shows two almost identical shots where on the left a peaked profile can be seen and on the right a hollow profile. The profiles are often elliptical, probably due to the magnetic fields present in the system.

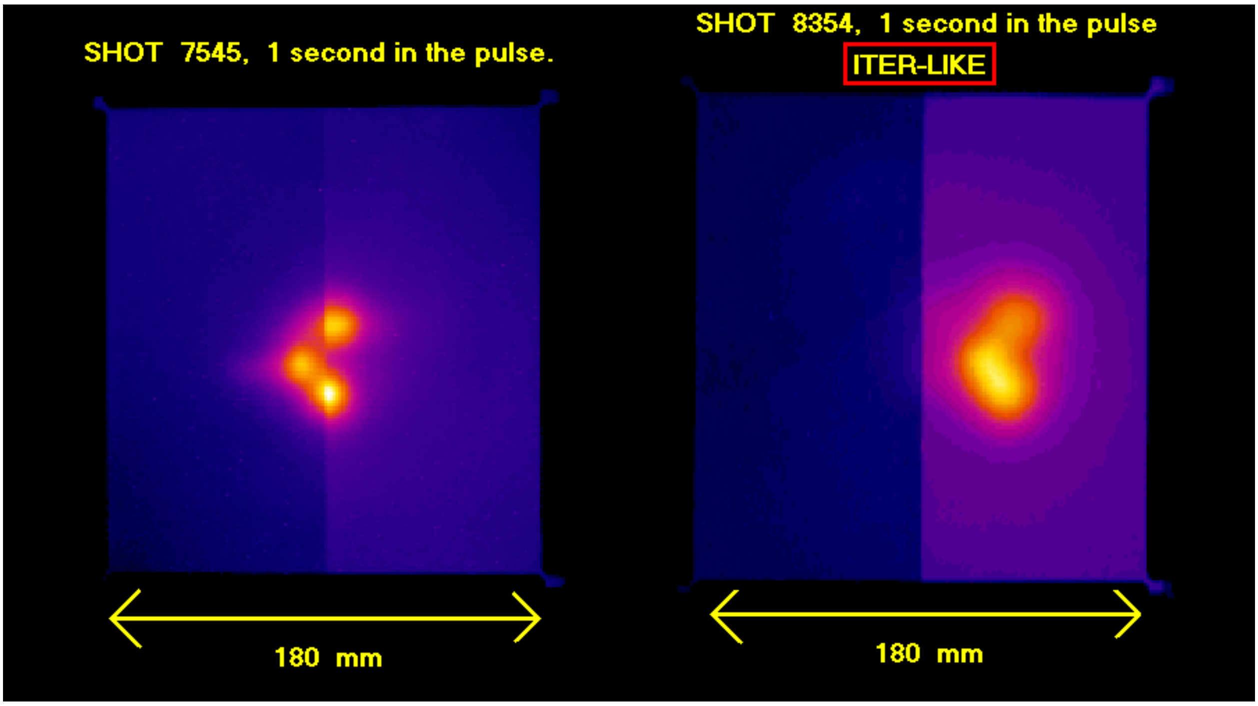

Figure 7. Displacing the anode aperture by 16 mm for a desired steering of +32 mm resulted in an actual steering of +32 mm (12 mrad). ITER needs ±10 mrad. The wider profile on the right is related to the beam optics, not to the anode displacement.

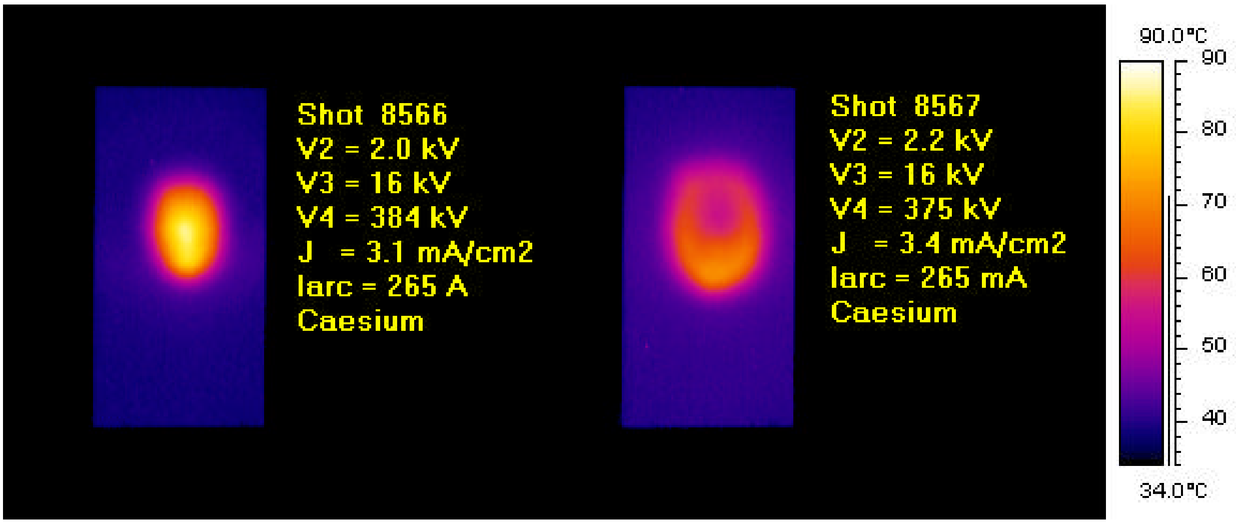

Figure 8. Two nearly identical shots in Caesium with very different beamlets are seen. On the left a normal peaked profile and on the right a hollow profile. The only difference is the extraction voltage that is 10 % higher in the case with the hollow profile.

10. Operation with a 6 mm gap between the plasma grid and the extraction grid

The ITER-like accelerator was designed to have a 3 mm gap between the plasma grid and the extraction grid. This is relatively short compared with the 14 mm diameter of the aperture in the plasma grid. The short gap was chosen in order to reduce the power of the intercepted co-extracted electrons since the extraction voltage could be kept to low values with a short gap. However during operation we found that the accelerator was very sensitive to small changes

in various parameters such as extraction voltage, bias and arc power. Therefore an experiment was done with a longer gap between the plasma grid and the extraction grid.
Before any caesium was introduced to the ion source a series of shots were done in «volume». The average of ten identical shots was taken and the vertical Gaussian fit was analyzed (shots 9625-9640). The pressure in the tank was lower in these shots compared with the shots described in section 4 above so the stripping losses are reduced. However the halo is still very similar to the shots obtained with the accelerator with 3 mm gap. See table 2.

Even if the operation time with the 6 mm gap has been very limited it was noted that triggering of hollow beams as mentioned in section 9 above could not be repeated. The beam profiles are as narrow as with the 3 mm gap and the halo's as mentioned above are very similar. See figure 9. One important feature though is that it is now possible to increase the current density to 150 A/m^2, which is 50 % higher than previously achieved with any SINGAP configuration. These high current densities could not be achieved at perveance match due to breakdowns in the main acceleration gap while increasing the beam energy above 580 kV. Figure 10 shows the performance of the "ITER-like" accelerator for all shots done since the new FLIR infrared camera was installed.

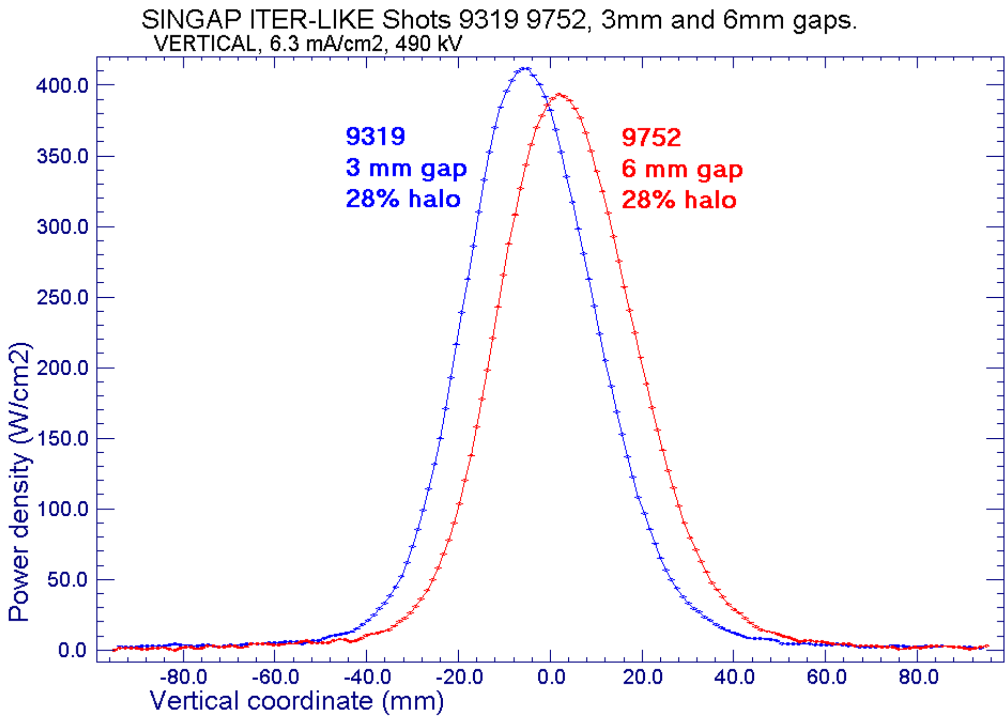

Figure 9. This plot shows a comparison of the vertical beam profiles for the two gaps, 3 and 6 mm between the plasma grid and the extraction grid. The profiles were measured with a FLIR 550 IR camera at the back of a graphite target.

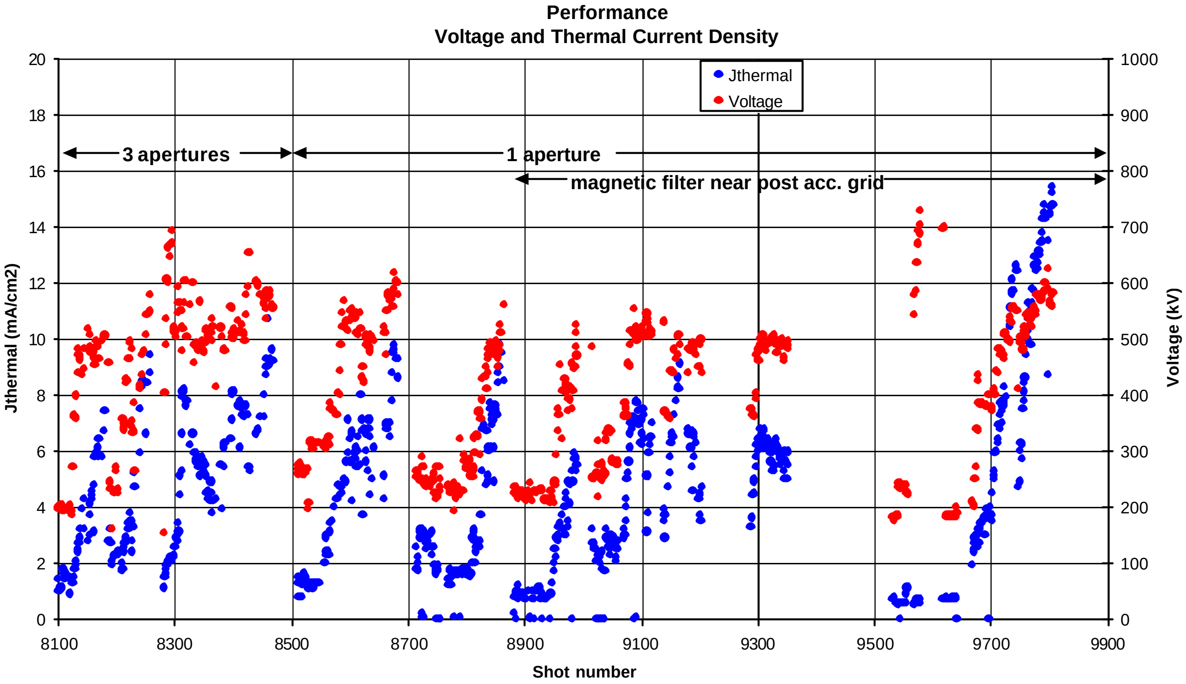

Figure 10. The performance of all shots measured with the Flir 550 infrared system. The shots after 9500 were done with 6 mm gap between the plasma grid and the extraction grid.

Conclusions

HV conditioning pulses have demonstrated that the ITER-like accelerator can hold 940 kV without breakdowns. D^- beams have been produced at 850 keV with a current density of 15 A/m^2 and with caesium at 580 keV with a current density of 150 A/m^2. This new record was performed after the gap between the plasma grid and the extraction grid was increased from 3 mm to 6 mm. The power is measured calorimetrically on the graphite target with an infrared camera.

The first experiments have so far confirmed some aspects of the design of the new ITER-like accelerator, but not all. In particular the experimental data show that the beamlets have a bi-Gaussian power density distribution (70% with a divergence of ≈4-5 mrad and 30% with a halo) as opposed to the single Gaussian with 2.5 mrad divergence of the simulation. The fraction of the total power that is seen as a halo varies between 15 % while operating at low current densities without Cs to 30 % during caesiated high current density operation with the positive ion suppression filter downstream of the SINGAP post acceleration grid. Without this filter the fraction of the power seen in the halo is increasing up to 40 %. A switch-on effect is also enhancing the halo for short pulses.

The accountability of the power is up to 90 % when operating at low tank pressure with the filter near the post acceleration grid and is reduced to 80 % without the filter. At high tank pressure a further decrease of the power accountability is seen. The difference due to pressure is, at least partly, caused by ionisation of background gas (by beams and back streaming positives). More positive ions can back stream in the absence of the magnetic filter at the post acceleration grid.

In the 3-beamlet configuration we found that the positions of the beamlets relative to each other are correct (within 1 mrad), except the central beamlet, which is almost 3 mrad too high. The reasons for these differences are not yet understood. Further experiments and simulations will be carried out in an attempt to understand the differences between the calculated and experimental beam profiles and the accelerated current density and the beam energy will be increased to as close as possible to 200 A/m^2 and 1 MeV.

Acknowledgement

The authors would like to thank UKAEA for the kindness of lending the Flir 550 infrared camera to us for these experiments.

References

1. L. Svensson, D. Boilson, H. P. L. de Esch, R. S. Hemsworth, A. Krylov and P. Massmann, Fusion Engineering and Design 66-68 (2003) 627-631
2. H. P. L. de Esch, R. S. Hemsworth and P. Massmann, *Updated physics design ITER-SINGAP accelerator*, submitted to Fusion Engineering and Design. Also presented at this conference
3. H.P.L. de Esch, R.S. Hemsworth, P. Massmann Design of the 1 MeV D- SINGAP accelerator for ITER neutral beam injection, this conference.
4. Y. Okumura, 18th International Conference on Fusion Energy, Sorrento, Italy, 4-10 October 2000.
5. P. Massmann, D. Boilson, H. P. L. de Esch, R. S. Hemsworth and L. Svensson, 20th ISDEIV, Tours, 2002
6. A. Krylov, R. S. Hemsworth, Gas losses and related beam losses in the ITER NBI, submitted to Fusion Engineering and Design.
7. H. P. L. de Esch, D Boilson, R S Hemsworth, P Massmann and L Svensson, Proc. 9th International Symposium on the Production and Neutralization of Negative Ions and Beams, Ed. Martin P Stockli, Gif-sur-Yvette, France 2002. AIP conference proceedings volume 639, pages 184-196.
8. ITER DDD5.3 http://132.169.11.26/iter-doc/ddd/ddd53/ddd53_index.html